Polystyrene microplastics induce an immunometabolic active state in macrophages

Seth Merkley
University of New Mexico Health Sciences Center
Harrison C Moss
University of New Mexico Health Sciences Center
Samuel M Goodfellow
University of New Mexico Health Sciences Center
Christina L Ling
University of New Mexico Health Sciences Center
Jewel L Meyer-Hagen
University of New Mexico Health Sciences Center
John Weaver
University of New Mexico Health Sciences Center
Matthew J Campen
University of New Mexico Health Sciences Center
Eliseo F Castillo (ecastillo@salud.unm.edu)
University of New Mexico Health Sciences Center https://orcid.org/0000-0002-5083-560X

Short Report

Keywords: microplastics, macrophage, metabolism, inflammation, particulates

Posted Date: February 22nd, 2021

DOI: https://doi.org/10.21203/rs.3.rs-259689/v1

Version of Record: A version of this preprint was published at Cell Biology and Toxicology on May 22nd, 2021. See the published version at https://doi.org/10.1007/s10565-021-09616-x.

Abstract

Anti- and pro-inflammatory responses in macrophages are influenced by cellular metabolism. Macrophages are the primary phagocyte in mucosal environments (*i.e.*, intestinal tract and lungs) acting as first-line defense against microorganisms and environmental pollutants. Given we now face extensive microplastic contamination of our food and water sources, we aimed to examine the metabolic response in macrophages to microplastic particles (MP). Utilizing murine macrophages, we assessed the metabolic response of macrophages after polystyrene MP phagocytosis. The phagocytosis of MP by macrophages induced a metabolic shift toward glycolysis and a reduction in mitochondrial respiration that was associated with an increase of cell surface markers CD80 and CD86 and cytokine gene expression associated with glycolysis. The gastrointestinal consequences of this metabolic switch in the context of an immune response remains uncertain but the global rise of plastic pollution and MP ingestion potentially pose an unappreciated health risk.

1. Introduction

Alarmingly, industrial microplastic particles (MP) have permeated global aquatic and terrestrial ecosystems (Wright and Kelly, 2017). We now face extensive MP contamination of our food and water sources, raising ecological and public health concerns (Cox et al., 2019). Human consumption of MP through our diet, although believed to be underestimated, is up to 142,000 particles annually; estimates increase to 211,000 particles when inhalation is considered (Cox et al., 2019; Koelmans et al., 2019; Novotna et al., 2019). Notably, these calculations are based on only 15% of the average Americans' caloric intake and do not account for numerous other sources of MP contamination including major food groups and food preparation, which can further contribute plastics to the diet (Cox et al., 2019). Polystyrene (PS), polyethylene (PE), polypropylene (PP), and polyethylene terephthalate (PET) make up more that 50% of microplastics found in the environment and the majority of the types of MP found in food(Catarino et al., 2018; Cau et al., 2019; Cheung et al., 2018; Cho et al., 2019; Doyen et al., 2019; Feng et al., 2019; Jahan et al., 2019; Karami et al., 2017a; Karami et al., 2017b; Kim et al., 2018; Li et al., 2015; Nan et al., 2020; Rummel et al., 2016; Tanaka and Takada, 2016; Wu et al., 2020). Thus, there is no debate we are ingesting and inhaling MP at increasing rates, but the human health impact remains unclear.

Several reports have shown MP accumulate in the gut and liver of mice after ingestion (Deng et al., 2017; Jin et al., 2019). Although the mechanism is unclear, MP exposure leads to gut dysbiosis, decreased mucin production, and localized liver inflammation (Deng et al., 2017; Jin et al., 2019; Lu et al., 2018). More recently, it was shown environmentally exposed MP enhances the uptake by macrophages(Ramsperger et al., 2020). Macrophages are the major phagocytic cell in both the liver and the intestinal tract and upon activation can contribute to inflammation-induced pathologies(Bain and Schridde, 2018; Bain et al., 2013; Wang et al., 2020). This cellular localization in mucosal environments allows macrophages to directly eliminate microbes upon barrier breakdown and to support the uptake of apoptotic barrier cells. Furthermore, macrophages as well as myeloid-derived dendritic cells in the lamina propria can sample the luminal content despite residing outside the lumen(Mazzini et al., 2014; Niess et

al., 2005). Through phagocytosis and macroautophagy (herein, referred to as autophagy), macrophages connect the intake of foreign materials to host immunity(Wu and Lu, 2019). Autophagy is a conserved catabolic process that degrades protein aggregates, damaged organelles and numerous pathogens (Galluzzi et al., 2017),(Gatica et al., 2018; Mizushima et al., 1998). The activation of autophagy has proven critical for macrophage function in response to stress and infection as well as providing energy during these functional states(Martinez et al., 2013).

Intestinal macrophages exhibit an anti-inflammatory phenotype under homeostatic conditions that allows them to function as highly phagocytic and bactericidal cells without initiating an inflammatory response (Bain and Schridde, 2018). A functional autophagic pathway in macrophages is critical for this anti-inflammatory phenotype(Lee et al., 2016; Merkley et al., 2020; Zhang et al., 2017). It is suggested that anti-inflammatory macrophages rely mainly on mitochondrial metabolism such as the oxidative phosphorylation (OXPHOS) and fatty acid oxidation for energy production(Diskin and Palsson-McDermott, 2018; Shanmugam et al., 2003). During inflammation, the macrophage niche changes – infiltrating monocytes differentiate into inflammatory macrophages capable of producing proinflammatory cytokines and promoting inflammation(Bain et al., 2013). This inflammatory phenotype is partly attributed to a glycolytic metabolic phenotype, which is called an immunometabolic active state (Diskin and Palsson-McDermott, 2018; Shanmugam et al., 2003). Glycolysis is also increased during phagocytosis(Newsholme et al., 1987; Schnyder and Baggiolini, 1978; Viola et al., 2019). During this metabolic switch, macrophages up-regulate cell surface markers such as CD80 and CD86 as well as cytokines such as IL-23 (Bain and Schridde, 2018; Diskin and Palsson-McDermott, 2018; Jha et al., 2015; Mogilenko et al., 2019). Thus, alterations in macrophage metabolism could have a significant impact on immunity and inflammation. In this brief report, we assessed the cellular response of macrophages to MP.

2. Methods

2.1 Cell culture and stimulation

Primary murine macrophages were generated as previously described(Castillo et al., 2012). Macrophages were stimulated with 10-µm polystyrene microplastics (Phosphorex, Cat# 118, 1 µg/mL).

2.2 Confocal Microscopy

Slide-adhered macrophages were treated with green fluorescent 10-µm polystyrene MP (Phosphorex, 2106G) for 4 hours in the presence or absence of Bafilomycin A1 (10nM) or pp242 (5µM). Slides were stained with LC3 (MBL Int.) and mounted with EMS ImmunoMount DAPI Mounting media (Cat# 17989-97). 1-3 µm Z-stack images were obtained using immunofluorescence at 1.6 Zoom by a 63X oil immersion objective. Images were processed using Zen Software and Adobe Photoshop (version CC 2019) and ImageJ was used for MFI analysis.

2.3 Flow Cytometry

Macrophages were pretreated with Stain FcX (anti-CD16/32) (Biolegend) before being stained for CD80 (Invitrogen) and CD86 (ThermoFisher). Mitochondria were stained with 100nM MitoTracker Green (Thermo, M7514) and 200nM MitoTracker Red CMXRos (Thermo, M22425) as previously reported(Castillo et al., 2012). Flow cytometry was carried out on the LSRFortessa (BD Biosciences) and data analyzed using FlowJo software (TreeStar).

2.4 Glycolytic Rate Assay (GRA)

Mitochondrial oxygen consumption rate (mitoOCR) and extracellular acidification rate (ECAR) were assayed in basal and MP groups via addition of Rotenone/Antimycin (Rot/AA, 0.5 μM), inhibiting mitochondrial electron transport chain complexes I and III, respectively, followed by 2-DG (50 mM), inhibiting hexokinase. mitoOCR and ECAR measurements were calculated via the GRA (Agilent #103344-100), and basal glycolysis, % proton efflux rate due to glycolysis (glycoPER), and mitoOCR/glycoPER ratios were obtained from the Seahorse XF Extracellular Flux Analyzer (Agilent Bioscience Inc).

2.5 RNA Isolation, Quantification, and RT-qPCR

RNA isolation was performed on cells stored in RNA-Later (Invitrogen) using the RNA Purelink Minikit (Invitrogen) according to the manufacturer's protocols. RNA was quantified on Nanodrop2000 and all samples yielded a 260/280 of 2 ± 0.15. cDNA synthesis was performed using Oligo(dT) Primer and SSIV Reverse Transcriptase in the presence of Cloned Ribonuclease Inhibitor (all ThermoFisher). Reverse transcription reaction and RT-qPCR runs utilized Taqman MasterMix (ThermoFisher) on a viiA7 Thermal Cycler (ThermoFisher) using QuantStudio 7. RT-qPCR primers and reagents used are listed in Table S1.

2.6. Statistical Analysis

Statistical analysis was performed as described in figure legends and graphs generated display mean (± SD) and were obtained using Prism software. Pearson's Correlation Coefficient was acquired from macrophages confocal images using Huygens's Deconvolution Scientific Volume Image Software (UNM Fluorescence Microscopy and Cell Imaging shared resource). All data were analyzed using two-tailed unpaired Student's t test (Prism) or One-Way ANOVA.

3. Results

3.1 Internalization of MP by macrophages does not result in MP degradation.

Utilizing fluorescently-labeled polystyrene MP (**Fig. 1A**), we investigated the uptake of MP by murine macrophages. Consistent with recent reports(Ramsperger et al., 2020; Stock et al., 2019), confocal microscopy revealed clear uptake of green fluorescent MP by macrophages (**Fig. 1B**). These internalized MP (green fluorescence) co-localized with the microtubule-associated proteins 1A/1B light chain 3 B (LC3, red fluorescence) (**Fig. 1C,D top row,** insets display enlarged puncta). LC3 is a key protein involved in internal cargo shuttling to autophagosomes in the autophagic pathway(Gatica et al., 2018; Mizushima et al., 1998) and LC3-associated phagocytosis (LAP)(Martinez et al., 2015; Sanjuan et al., 2007). LAP is a

phagocytic immune activating mechanism that utilizes cell surface LC3 to phagocytose extracellular cargo. To determine if the autophagy pathway could degrade the internalized MP, we activated autophagy in macrophages after MP internalization with the mTOR inhibitor, Torkinib (pp242)(Zeng et al., 2012). Interestingly, LC3 (red) and MP (green) still co-localized (**Fig. 1C,D middle row**) in macrophages after the induction of autophagy albeit at a significantly lower level than in unstimulated macrophages. The presence of co-localized LC3 and MP after autophagy induction suggests macrophage autophagy cannot completely clear MP.

To determine if autophagy or LAP are required for MP internalization, we utilized Bafilomycin A1 (Baf.A1), a specific inhibitor of the vacuolar-type H^+-ATPase(Florey et al., 2015; Yoshimori et al., 1991). Baf.A1 can prevent LAP (Gao et al., 2016) as well as block the final step of autophagy (preventing degradation of the autophagosomal contents and allows accumulation of LC3-bound cargo)(Yoshimori et al., 1991). Upon Baf. A1 stimulation there was minimal to no co-localization of MP (green) and LC3 (red) (**Fig. 1C,D bottom row**) compared to autophagy induction (**Fig. 1D**). Interestingly, MP were still internalized by macrophages (**Fig. 1C bottom row**). Utilizing macrophages from mice with an *Atg5*-deficiency in myeloid cells(Castillo et al., 2012; Zhao et al., 2008), we examined if *Atg5*-deficient macrophages could still phagocytose MP. Atg5 is involved in multiple steps in the autophagic process (Hanada et al., 2007; Mizushima et al., 1998; Noda et al., 2013; Sakoh-Nakatogawa et al., 2013) as well as LAP (Heckmann et al., 2019). In comparison to wild-type macrophages, the fluorescence intensity of intracellular MP was not significantly different compared to *Atg5*-deficient macrophages suggesting no change in the amount of MP internalization (**Fig. 1E**). In the absence or presence of Baf.A1, *Atg5*-deficient macrophages were still capable of MP phagocytosis (**Fig. 1F**). Overall, our results suggest macrophages can phagocytose MP in both LAP-dependent and –independent mechanisms; however, neither mechanism can completely degrade MP.

3.2 MP phagocytosis by macrophages biases them toward a less oxidative, more glycolytic metabolic profile

The phagocytosis of external cargo by macrophages can have profound effects on immune activation(Schnyder and Baggiolini, 1978). Currently, it is unclear how macrophages respond to MP, and as MP are not completely degraded by autophagy, they may provide an extended challenge to macrophage homeostasis. Therefore, we examined the cellular response of macrophages to MP. Interestingly, MP internalization significantly increased cell surface expression of two major co-stimulatory molecules, CD80 (**Fig. 2A,B**) and CD86 (**Fig. 2C,D**) relative to unstimulated macrophages. Furthermore, *Il23p19* (**Fig. 2E**) and *Il12p40* (**Fig. 2F**), the genes comprising the proinflammatory cytokine IL-23, also showed elevated expression after MP internalization. No change was observed for anti-inflammatory cytokines *Il10* (**Fig. 2G**) or *Tgfb1* (**Fig. 2H**).

Phagocytosis can lead to the upregulation of co-stimulatory molecules. During phagocytosis, the glycolytic pathway is upregulated which is crucial for CD80 and CD86 upregulation (Bain and Schridde, 2018; Diskin and Palsson-McDermott, 2018; Jha et al., 2015; Mogilenko et al., 2019; Newsholme et al., 1987; Schnyder and Baggiolini, 1978; Viola et al., 2019). As mentioned above, glycolysis is closely linked to an inflammatory state in macrophages, as many glycolytic enzymes serve to directly enhance inflammation(Millet et al., 2016; Palsson-McDermott et al., 2017; Xie et al., 2016).Thus, we examined the extracellular acidification rate (ECAR) and proton efflux rate (PER) as measurements of glycolysis and mitochondrial/TCA cycle activity in macrophages at a basal state, stimulated with MP as well as low-dose lipopolysaccharide (LPS, 100 pg/mL) stimulation and MP plus LPS stimulation. The kinetics for oxygen consumption rate (OCR), PER, and ECAR of basal and MP stimulated macrophages (**Fig. 2I-K**) are shown for simplification. Basal state and low-dose LPS stimulated macrophages were highly oxidative (**Fig. 2L-O**), but all treatments showed indistinguishable compensatory glycolysis responses upon mitochondrial inhibition (**Fig. 2M**). After the phagocytosis of MP in the absence or presence of LPS, macrophages showed a more glycolytic biased phenotype, indicated by higher basal glycolysis (**Fig. 2L**), reduced mitochondrial metabolism as shown by a lower mitoOCR/glyoPER ratio (**Fig. 2O**), and the majority of PER due to glycolysis (**Fig. 2N**). Further analysis of MP stimulated macrophages revealed a decrease in mitochondrial membrane potential as determined by decreased Mitotracker Red CMXRos staining in MP stimulated macrophages (**Fig. 2P, Q**). Collectively, our data suggest the phagocytosis of MP by macrophages can induce an immunometabolic active state.

4. Discussion

In summary, we found after the phagocytosis of MP by macrophages, MP could not be fully degraded in the observed timescale, and this internalization induces an immunometabolically active phenotype in macrophages. Specifically, resting macrophages in a metabolic oxidative state became more glycolytic after MP phagocytosis. This shift toward glycolysis came at the expense of maintaining mitochondrial respiration. Ultimately, this switch in cellular metabolism increased cell surface co-stimulatory molecules CD80 and CD86 and upregulated proinflammatory cytokine genes.

The *in vivo* consequence of macrophages phagocytosing MP is unclear. MP have been found in human feces, suggesting that humans are ingesting MP(Schwabl et al., 2019). Autophagy and phagocytosis are crucial immunological functions utilized by macrophages to remove pathogens, apoptotic cells or cellular debris to maintain cellular and tissue homeostasis. Intestinal macrophages could likely uptake MP at numerous sites in the GI tract including sampling the lumen(Mazzini et al., 2014), paracellular persorption at the gut epithelium (for particles <130 μm)(Wright and Kelly, 2017), and trafficking through ileal Peyer's patches via M-cells(Knoop et al., 2013). While the presence of MP alone may not be enough to induce substantial inflammatory activation, the daily introduction of MP into the human GI tract exposes MP to a plethora of microorganisms which could contribute to the gut and liver inflammation observed in animals ingesting MP. The uptake of MP laden with microorganisms by lamina propria phagocytes could introduce a bias toward low-grade inflammation and likely exacerbates pre-existing pathologies in the gut and surrounding tissues.

The exposure of MP to the GI tract puts barrier cells in contact with these environmental pollutants. Phagocytosis can also occur in barrier cells such as intestinal and respiratory epithelial cells and MP have been shown to be phagocytosed by colonocytes(Stock et al., 2019). Given the high consumption of MP in industrialized nations, it is concerning that the phagocytosis of MP altered macrophage metabolism. An oxidative metabolic state in differentiated intestinal epithelial cells (IEC) is crucial for intestinal homeostasis(Litvak et al., 2018). IEC rely on OXPHOS and fatty acid oxidation for the highly energy-dependent regulation of tight junction proteins that are critical for maintaining the barrier and reducing intestinal permeability(Litvak et al., 2018). Inhibitors of the H^+ gradient, dinitrophenol and sodium azide, have been shown to induce IP(Litvak et al., 2018; Ma et al., 1999) . Additionally, IEC sequester oxygen during mitochondrial metabolism(Litvak et al., 2018). This prevents oxygen from crossing the barrier and subsequently preserves an obligate anaerobic microbial community. Thus, MP-induced changes in IEC metabolism could have a significant impact on gut health. Notably, the incidence of inflammatory bowel disease (IBD), a chronic and remitting disease of the GI tract, in western countries rose rapidly in the latter part of the 20^{th} century, in parallel with plastic pollution, and is now becoming a global epidemic(Ng et al., 2018). Although the incidence of IBD in North America and Europe have begun to stabilize, the prevalence of IBD in these western nations has increased dramatically; the cause of which remains unknown. Moreover, most models do not account for environmental impact on IBD and no studies have been specifically conducted to confirm a role for MP in inducing or exacerbating IBD(Zhao and Burisch, 2019). Given the parallels with the rates of MP ingestion, there is ample justification to study whether MP contribute to this global epidemic.

Abbreviations

ECAR: Extracellular acidification rate

GRA: Glycolytic Rate Assay

IBD: Inflammatory bowel disease

IEC: Intestinal epithelial cell

LAP: LC3-associated phagocytosis

MFI: mean fluorescence intensity

mitoOCR: Mitochondrial oxygen consumption rate

MP: Microplastic particles

PER: Proton efflux rate

TCA: Tricarboxylic acid cycle

Declarations

Author Contributions

SDM participated in writing the manuscript and performed all experiments with help from HCM, JMH, CLL and JW. SMG performed confocal microscopy. MJC provided critical reagents and helped design the study. EFC designed the study, analyzed data, and wrote the paper. All authors approved the final version of the manuscript.

Acknowledgments, Funding and Disclosures

Supported in part by the National Center for Research Resources and the National Center for Advancing Translational Sciences of the National Institutes of Health (NIH) through grant no. UL1TR001449 (E.F.C.), in part by NIH grant P20GM121176 (E.F.C.), P20GM130422 (M.J.C) and New Mexico Medical Trust C-2446-RAC (E.F.C.). S.M.G. was supported in part by the Infectious Disease and Inflammation Program Pre-doctoral T32 training grant, NIH/NIAID grant T32AI007538. The authors declare no conflict of interest.

Declaration of Competing Interest

The authors declare no conflict of interest.

Ethics approval (include appropriate approvals or waivers)

All experiments were approved by the Institutional Animal Care and Use Committee of the University of New Mexico Health Sciences Center, in accordance with the National Institutes of Health guidelines for use of live animals. The University of New Mexico Health Sciences Center is accredited by the American Association for Accreditation of Laboratory Animal Care.

Consent to participate (include appropriate statements)

'Not applicable'

Consent for publication (include appropriate statements)

'Not applicable'

Availability of data and material (data transparency)

'Not applicable'

Code availability (software application or custom code)

'Not applicable'

References

Bain, C.C., and Schridde, A. (2018). Origin, Differentiation, and Function of Intestinal Macrophages. Front Immunol *9*, 2733.

Bain, C.C., Scott, C.L., Uronen-Hansson, H., Gudjonsson, S., Jansson, O., Grip, O., Guilliams, M., Malissen, B., Agace, W.W., and Mowat, A.M. (2013). Resident and pro-inflammatory macrophages in the colon represent alternative context-dependent fates of the same Ly6Chi monocyte precursors. Mucosal Immunol *6*, 498-510.

Castillo, E.F., Dekonenko, A., Arko-Mensah, J., Mandell, M.A., Dupont, N., Jiang, S., Delgado-Vargas, M., Timmins, G.S., Bhattacharya, D., Yang, H.*, et al.* (2012). Autophagy protects against active tuberculosis by suppressing bacterial burden and inflammation. Proc Natl Acad Sci U S A *109*, E3168-3176.

Catarino, A.I., Macchia, V., Sanderson, W.G., Thompson, R.C., and Henry, T.B. (2018). Low levels of microplastics (MP) in wild mussels indicate that MP ingestion by humans is minimal compared to exposure via household fibres fallout during a meal. Environ Pollut *237*, 675-684.

Cau, A., Avio, C.G., Dessi, C., Follesa, M.C., Moccia, D., Regoli, F., and Pusceddu, A. (2019). Microplastics in the crustaceans Nephrops norvegicus and Aristeus antennatus: Flagship species for deep-sea environments? Environ Pollut *255*, 113107.

Cheung, L.T.O., Lui, C.Y., and Fok, L. (2018). Microplastic Contamination of Wild and Captive Flathead Grey Mullet (Mugil cephalus). Int J Environ Res Public Health *15*.

Cho, Y., Shim, W.J., Jang, M., Han, G.M., and Hong, S.H. (2019). Abundance and characteristics of microplastics in market bivalves from South Korea. Environ Pollut *245*, 1107-1116.

Cox, K.D., Covernton, G.A., Davies, H.L., Dower, J.F., Juanes, F., and Dudas, S.E. (2019). Human Consumption of Microplastics. Environ Sci Technol *53*, 7068-7074.

Deng, Y., Zhang, Y., Lemos, B., and Ren, H. (2017). Tissue accumulation of microplastics in mice and biomarker responses suggest widespread health risks of exposure. Sci Rep *7*, 46687.

Diskin, C., and Palsson-McDermott, E.M. (2018). Metabolic Modulation in Macrophage Effector Function. Front Immunol *9*, 270.

Doyen, P., Hermabessiere, L., Dehaut, A., Himber, C., Decodts, M., Degraeve, T., Delord, L., Gaboriaud, M., Mone, P., Sacco, J.*, et al.* (2019). Occurrence and identification of microplastics in beach sediments from the Hauts-de-France region. Environ Sci Pollut Res Int *26*, 28010-28021.

Feng, Z., Zhang, T., Li, Y., He, X., Wang, R., Xu, J., and Gao, G. (2019). The accumulation of microplastics in fish from an important fish farm and mariculture area, Haizhou Bay, China. Sci Total Environ *696*, 133948.

Florey, O., Gammoh, N., Kim, S.E., Jiang, X., and Overholtzer, M. (2015). V-ATPase and osmotic imbalances activate endolysosomal LC3 lipidation. Autophagy *11*, 88-99.

Galluzzi, L., Baehrecke, E.H., Ballabio, A., Boya, P., Bravo-San Pedro, J.M., Cecconi, F., Choi, A.M., Chu, C.T., Codogno, P., Colombo, M.I.*, et al.* (2017). Molecular definitions of autophagy and related processes. EMBO J *36*, 1811-1836.

Gao, Y., Liu, Y., Hong, L., Yang, Z., Cai, X., Chen, X., Fu, Y., Lin, Y., Wen, W., Li, S.*, et al.* (2016). Golgi-associated LC3 lipidation requires V-ATPase in noncanonical autophagy. Cell Death Dis *7*, e2330.

Gatica, D., Lahiri, V., and Klionsky, D.J. (2018). Cargo recognition and degradation by selective autophagy. Nat Cell Biol *20*, 233-242.

Hanada, T., Noda, N.N., Satomi, Y., Ichimura, Y., Fujioka, Y., Takao, T., Inagaki, F., and Ohsumi, Y. (2007). The Atg12-Atg5 conjugate has a novel E3-like activity for protein lipidation in autophagy. J Biol Chem *282*, 37298-37302.

Heckmann, B.L., Teubner, B.J.W., Tummers, B., Boada-Romero, E., Harris, L., Yang, M., Guy, C.S., Zakharenko, S.S., and Green, D.R. (2019). LC3-Associated Endocytosis Facilitates beta-Amyloid Clearance and Mitigates Neurodegeneration in Murine Alzheimer's Disease. Cell *178*, 536-551 e514.

Jahan, S., Strezov, V., Weldekidan, H., Kumar, R., Kan, T., Sarkodie, S.A., He, J., Dastjerdi, B., and Wilson, S.P. (2019). Interrelationship of microplastic pollution in sediments and oysters in a seaport environment of the eastern coast of Australia. Sci Total Environ *695*, 133924.

Jha, A.K., Huang, S.C., Sergushichev, A., Lampropoulou, V., Ivanova, Y., Loginicheva, E., Chmielewski, K., Stewart, K.M., Ashall, J., Everts, B.*, et al.* (2015). Network integration of parallel metabolic and transcriptional data reveals metabolic modules that regulate macrophage polarization. Immunity *42*, 419-430.

Jin, Y., Lu, L., Tu, W., Luo, T., and Fu, Z. (2019). Impacts of polystyrene microplastic on the gut barrier, microbiota and metabolism of mice. Sci Total Environ *649*, 308-317.

Karami, A., Golieskardi, A., Ho, Y.B., Larat, V., and Salamatinia, B. (2017a). Microplastics in eviscerated flesh and excised organs of dried fish. Sci Rep *7*, 5473.

Karami, A., Golieskardi, A., Keong Choo, C., Larat, V., Galloway, T.S., and Salamatinia, B. (2017b). The presence of microplastics in commercial salts from different countries. Sci Rep *7*, 46173.

Kim, J.S., Lee, H.J., Kim, S.K., and Kim, H.J. (2018). Global Pattern of Microplastics (MPs) in Commercial Food-Grade Salts: Sea Salt as an Indicator of Seawater MP Pollution. Environ Sci Technol *52*, 12819-12828.

Knoop, K.A., Miller, M.J., and Newberry, R.D. (2013). Transepithelial antigen delivery in the small intestine: different paths, different outcomes. Curr Opin Gastroenterol *29*, 112-118.

Koelmans, A.A., Mohamed Nor, N.H., Hermsen, E., Kooi, M., Mintenig, S.M., and De France, J. (2019). Microplastics in freshwaters and drinking water: Critical review and assessment of data quality. Water Res *155*, 410-422.

Lee, H.Y., Kim, J., Quan, W., Lee, J.C., Kim, M.S., Kim, S.H., Bae, J.W., Hur, K.Y., and Lee, M.S. (2016). Autophagy deficiency in myeloid cells increases susceptibility to obesity-induced diabetes and experimental colitis. Autophagy *12*, 1390-1403.

Li, J., Yang, D., Li, L., Jabeen, K., and Shi, H. (2015). Microplastics in commercial bivalves from China. Environ Pollut *207*, 190-195.

Litvak, Y., Byndloss, M.X., and Baumler, A.J. (2018). Colonocyte metabolism shapes the gut microbiota. Science *362*.

Lu, L., Wan, Z., Luo, T., Fu, Z., and Jin, Y. (2018). Polystyrene microplastics induce gut microbiota dysbiosis and hepatic lipid metabolism disorder in mice. Sci Total Environ *631-632*, 449-458.

Ma, T.Y., Nguyen, D., Bui, V., Nguyen, H., and Hoa, N. (1999). Ethanol modulation of intestinal epithelial tight junction barrier. Am J Physiol *276*, G965-974.

Martinez, J., Malireddi, R.K., Lu, Q., Cunha, L.D., Pelletier, S., Gingras, S., Orchard, R., Guan, J.L., Tan, H., Peng, J.*, et al.* (2015). Molecular characterization of LC3-associated phagocytosis reveals distinct roles for Rubicon, NOX2 and autophagy proteins. Nat Cell Biol *17*, 893-906.

Martinez, J., Verbist, K., Wang, R., and Green, D.R. (2013). The relationship between metabolism and the autophagy machinery during the innate immune response. Cell Metab *17*, 895-900.

Mazzini, E., Massimiliano, L., Penna, G., and Rescigno, M. (2014). Oral tolerance can be established via gap junction transfer of fed antigens from CX3CR1(+) macrophages to CD103(+) dendritic cells. Immunity *40*, 248-261.

Merkley, S.D., Goodfellow, S.M., Guo, Y., Wilton, Z.E.R., Byrum, J.R., Schwalm, K.C., Dinwiddie, D.L., Gullapalli, R.R., Deretic, V., Hernandez, A.J.*, et al.* (2020). Non-autophagy role of Atg5 and NBR1 in unconventional secretion of IL-12 prevents gut dysbiosis and inflammation. bioRxiv, 2020.2012.2007.414227.

Millet, P., Vachharajani, V., McPhail, L., Yoza, B., and McCall, C.E. (2016). GAPDH Binding to TNF-alpha mRNA Contributes to Posttranscriptional Repression in Monocytes: A Novel Mechanism of Communication between Inflammation and Metabolism. J Immunol *196*, 2541-2551.

Mizushima, N., Noda, T., Yoshimori, T., Tanaka, Y., Ishii, T., George, M.D., Klionsky, D.J., Ohsumi, M., and Ohsumi, Y. (1998). A protein conjugation system essential for autophagy. Nature *395*, 395-398.

Mogilenko, D.A., Haas, J.T., L'Homme, L., Fleury, S., Quemener, S., Levavasseur, M., Becquart, C., Wartelle, J., Bogomolova, A., Pineau, L.*, et al.* (2019). Metabolic and Innate Immune Cues Merge into a Specific Inflammatory Response via the UPR. Cell *178*, 263.

Nan, B., Su, L., Kellar, C., Craig, N.J., Keough, M.J., and Pettigrove, V. (2020). Identification of microplastics in surface water and Australian freshwater shrimp Paratya australiensis in Victoria, Australia. Environ Pollut *259*, 113865.

Newsholme, P., Gordon, S., and Newsholme, E.A. (1987). Rates of utilization and fates of glucose, glutamine, pyruvate, fatty acids and ketone bodies by mouse macrophages. Biochem J *242*, 631-636.

Ng, S.C., Shi, H.Y., Hamidi, N., Underwood, F.E., Tang, W., Benchimol, E.I., Panaccione, R., Ghosh, S., Wu, J.C.Y., Chan, F.K.L.*, et al.* (2018). Worldwide incidence and prevalence of inflammatory bowel disease in the 21st century: a systematic review of population-based studies. Lancet *390*, 2769-2778.

Niess, J.H., Brand, S., Gu, X., Landsman, L., Jung, S., McCormick, B.A., Vyas, J.M., Boes, M., Ploegh, H.L., Fox, J.G.*, et al.* (2005). CX3CR1-mediated dendritic cell access to the intestinal lumen and bacterial clearance. Science *307*, 254-258.

Noda, N.N., Fujioka, Y., Hanada, T., Ohsumi, Y., and Inagaki, F. (2013). Structure of the Atg12-Atg5 conjugate reveals a platform for stimulating Atg8-PE conjugation. EMBO Rep *14*, 206-211.

Novotna, K., Cermakova, L., Pivokonska, L., Cajthaml, T., and Pivokonsky, M. (2019). Microplastics in drinking water treatment - Current knowledge and research needs. Sci Total Environ *667*, 730-740.

Palsson-McDermott, E.M., Dyck, L., Zaslona, Z., Menon, D., McGettrick, A.F., Mills, K.H.G., and O'Neill, L.A. (2017). Pyruvate Kinase M2 Is Required for the Expression of the Immune Checkpoint PD-L1 in Immune Cells and Tumors. Front Immunol *8*, 1300.

Ramsperger, A., Narayana, V.K.B., Gross, W., Mohanraj, J., Thelakkat, M., Greiner, A., Schmalz, H., Kress, H., and Laforsch, C. (2020). Environmental exposure enhances the internalization of microplastic particles into cells. Sci Adv *6*.

Rummel, C.D., Loder, M.G., Fricke, N.F., Lang, T., Griebeler, E.M., Janke, M., and Gerdts, G. (2016). Plastic ingestion by pelagic and demersal fish from the North Sea and Baltic Sea. Mar Pollut Bull *102*, 134-141.

Sakoh-Nakatogawa, M., Matoba, K., Asai, E., Kirisako, H., Ishii, J., Noda, N.N., Inagaki, F., Nakatogawa, H., and Ohsumi, Y. (2013). Atg12-Atg5 conjugate enhances E2 activity of Atg3 by rearranging its catalytic site. Nat Struct Mol Biol *20*, 433-439.

Sanjuan, M.A., Dillon, C.P., Tait, S.W., Moshiach, S., Dorsey, F., Connell, S., Komatsu, M., Tanaka, K., Cleveland, J.L., Withoff, S.*, et al.* (2007). Toll-like receptor signalling in macrophages links the autophagy pathway to phagocytosis. Nature *450*, 1253-1257.

Schnyder, J., and Baggiolini, M. (1978). Role of phagocytosis in the activation of macrophages. J Exp Med *148*, 1449-1457.

Schwabl, P., Koppel, S., Konigshofer, P., Bucsics, T., Trauner, M., Reiberger, T., and Liebmann, B. (2019). Detection of Various Microplastics in Human Stool: A Prospective Case Series. Ann Intern Med *171*, 453-457.

Shanmugam, N., Reddy, M.A., Guha, M., and Natarajan, R. (2003). High glucose-induced expression of proinflammatory cytokine and chemokine genes in monocytic cells. Diabetes *52*, 1256-1264.

Stock, V., Bohmert, L., Lisicki, E., Block, R., Cara-Carmona, J., Pack, L.K., Selb, R., Lichtenstein, D., Voss, L., Henderson, C.J.*, et al.* (2019). Uptake and effects of orally ingested polystyrene microplastic particles in vitro and in vivo. Arch Toxicol *93*, 1817-1833.

Tanaka, K., and Takada, H. (2016). Microplastic fragments and microbeads in digestive tracts of planktivorous fish from urban coastal waters. Sci Rep *6*, 34351.

Viola, A., Munari, F., Sanchez-Rodriguez, R., Scolaro, T., and Castegna, A. (2019). The Metabolic Signature of Macrophage Responses. Front Immunol *10*, 1462.

Wang, X., Rao, H., Zhao, J., Wee, A., Li, X., Fei, R., Huang, R., Wu, C., Liu, F., and Wei, L. (2020). STING expression in monocyte-derived macrophages is associated with the progression of liver inflammation and fibrosis in patients with nonalcoholic fatty liver disease. Lab Invest *100*, 542-552.

Wright, S.L., and Kelly, F.J. (2017). Plastic and Human Health: A Micro Issue? Environ Sci Technol *51*, 6634-6647.

Wu, F., Wang, Y., Leung, J.Y.S., Huang, W., Zeng, J., Tang, Y., Chen, J., Shi, A., Yu, X., Xu, X.*, et al.* (2020). Accumulation of microplastics in typical commercial aquatic species: A case study at a productive aquaculture site in China. Sci Total Environ *708*, 135432.

Wu, M.Y., and Lu, J.H. (2019). Autophagy and Macrophage Functions: Inflammatory Response and Phagocytosis. Cells *9*.

Xie, M., Yu, Y., Kang, R., Zhu, S., Yang, L., Zeng, L., Sun, X., Yang, M., Billiar, T.R., Wang, H.*, et al.* (2016). PKM2-dependent glycolysis promotes NLRP3 and AIM2 inflammasome activation. Nat Commun *7*, 13280.

Yoshimori, T., Yamamoto, A., Moriyama, Y., Futai, M., and Tashiro, Y. (1991). Bafilomycin A1, a specific inhibitor of vacuolar-type H(+)-ATPase, inhibits acidification and protein degradation in lysosomes of

cultured cells. J Biol Chem *266*, 17707-17712.

Zeng, Z., Shi, Y.X., Tsao, T., Qiu, Y., Kornblau, S.M., Baggerly, K.A., Liu, W., Jessen, K., Liu, Y., Kantarjian, H.*, et al.* (2012). Targeting of mTORC1/2 by the mTOR kinase inhibitor PP242 induces apoptosis in AML cells under conditions mimicking the bone marrow microenvironment. Blood *120*, 2679-2689.

Zhang, H., Zheng, L., McGovern, D.P., Hamill, A.M., Ichikawa, R., Kanazawa, Y., Luu, J., Kumagai, K., Cilluffo, M., Fukata, M.*, et al.* (2017). Myeloid ATG16L1 Facilitates Host-Bacteria Interactions in Maintaining Intestinal Homeostasis. J Immunol *198*, 2133-2146.

Zhao, M., and Burisch, J. (2019). Impact of Genes and the Environment on the Pathogenesis and Disease Course of Inflammatory Bowel Disease. Dig Dis Sci *64*, 1759-1769.

Zhao, Z., Fux, B., Goodwin, M., Dunay, I.R., Strong, D., Miller, B.C., Cadwell, K., Delgado, M.A., Ponpuak, M., Green, K.G.*, et al.* (2008). Autophagosome-independent essential function for the autophagy protein Atg5 in cellular immunity to intracellular pathogens. Cell Host Microbe *4*, 458-469.

Figures

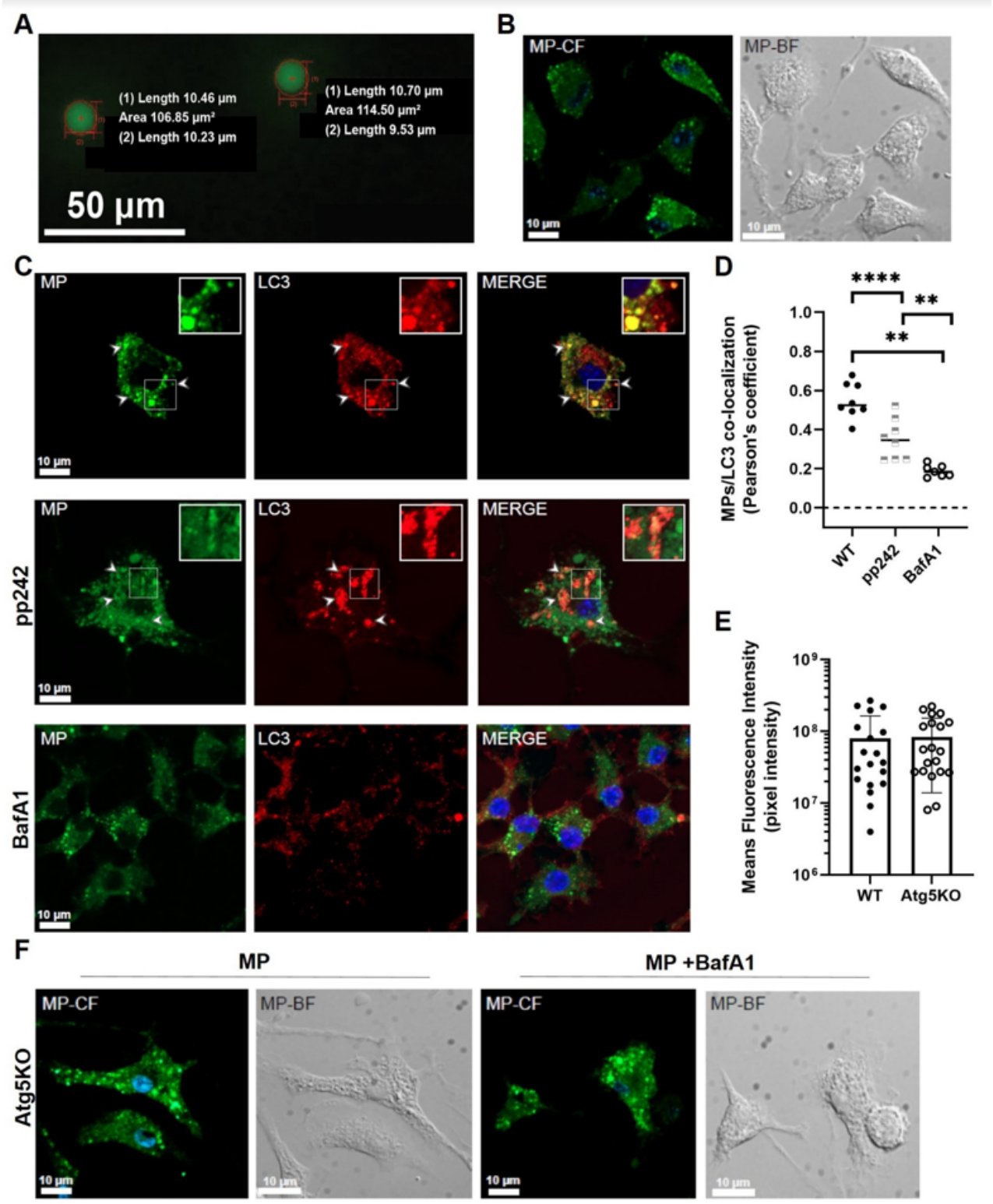

Figure 1

Macrophages utilize LC3-associated phagocytosis to uptake MP. 1-3 µm Z-stack images were performed on macrophages using immunofluorescence at 1.6 Zoom by a 63X oil immersion objective. (A) 10-micron MP were visualized and measured pre-exposure to macrophages. Representative from 5 images. Scale bar: 50 µm. (B) Macrophages were visualized for fluorescent MP using confocal (CF) and brightfield (BF) imaging. Representative from 20 images from 4 slides. (C) Macrophages were visualized for fluorescent

MP co-localization with LC3 in the absence or presence of Baf. A1 (10nM) or pp242 (5μM). Arrows indicate puncta displaying co-localization Insets. Representative from 15 images from 4 slides. Scale bars: 10 μm. (D) Quantification of MP/LC3 co-localization using Pearson's correlation coefficient (colocalization) and unpaired Student's t-test. Graph indicates mean *** indicates a p-value<0.001 (t-test). (E) Graph displaying the Mean fluorescence intensity (MFI) of MP fluorescence and uptake in macrophages. Each dot represents an image with a total of 20 images for each condition. (F) Atg5KO macrophages with or without Baf. A1 were visualized for MP uptake using confocal (CF) and brightfield (BF). Representative from 20 images from 5 slides. Scale bars: 10 μm.

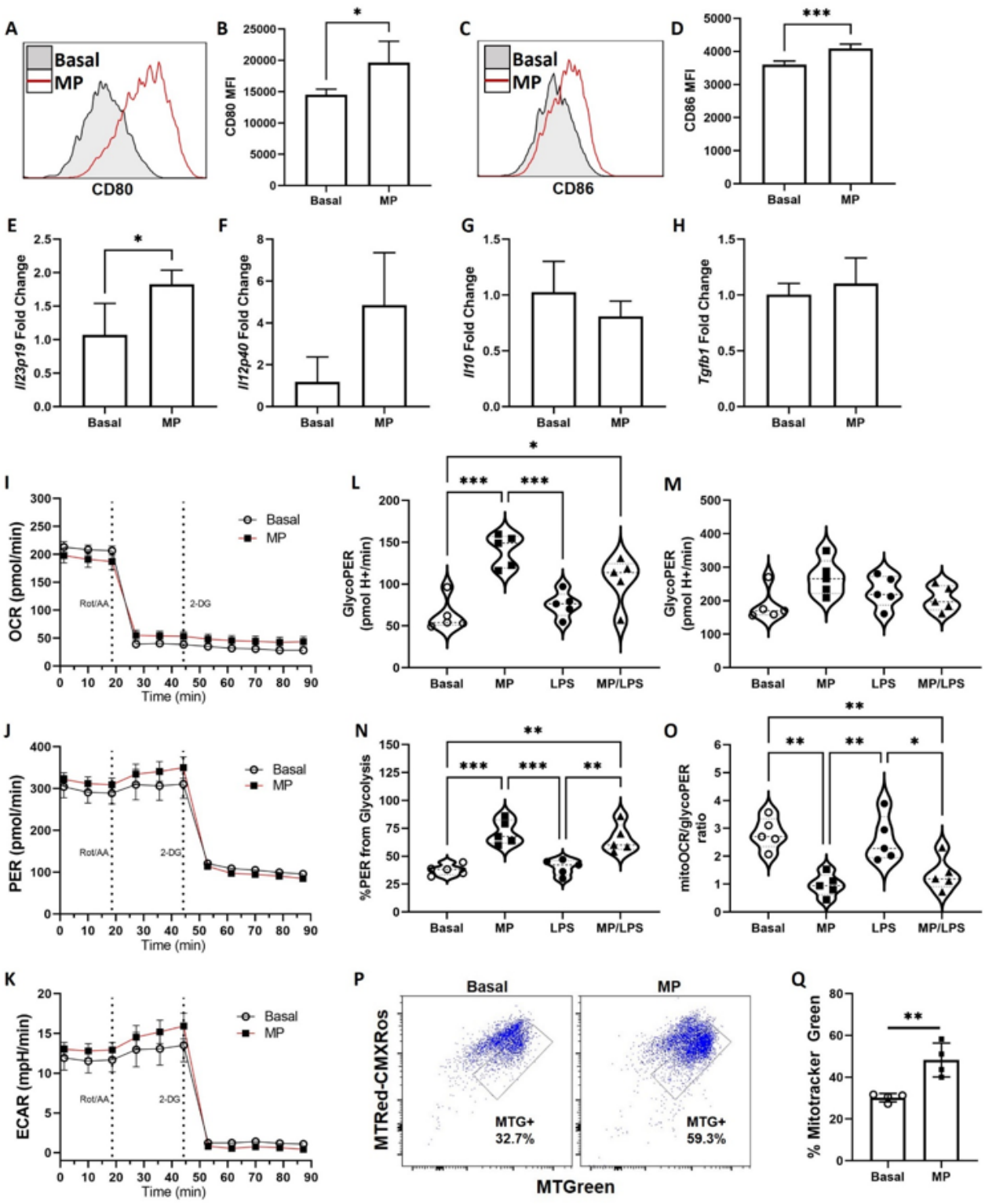

Figure 2

Microplastics induce a glycolytic shift in macrophages. (A) Representative histograms of cell surface expression of CD80 between basal (gray) and MP stimulated macrophages (red). (B) Graph displaying the Mean fluorescence intensity (MFI) of CD80 cell surface expression in both macrophage conditions. (C) Representative histograms of cell surface expression of CD86 between basal (gray) and MP stimulated macrophages (red). (D) Graph displaying the MFI of CD86 cell surface expression in both

macrophage conditions. (E-H) RT-qPCR data showing relative fold changes (2^-ddCT) in cytokine mRNA expression of bone marrow macrophages treated with 1 ug/mL of PS overnight. (E) Il23p19, (F) Il12p40 (G) Il10, (H) Tgfb1. For I-K, macrophages were plated (105 cells/well) in a XF24 cell culture microplate for 16 hours with complete media ±MP. Cells were assayed for (I) Oxygen consumption rate (OCR), (J) Proton efflux rate (PER), and (K) Extracellular acidification rate (ECAR) at regular increments throughout the experiment, with the timing of sequential drug additions indicated. Macrophages stimulated with MP showed a higher glycolytic phenotype as indicated by graphs displaying (L) higher basal glycolysis, (M) compensatory glycolysis, (N) a higher % of PER from glycolysis, and (O) a lower mitoOCR/glycoPER basal ratio. (P) Representative flow cytometric plots of mitochondrial membrane potential assessed by staining macrophages with MitoTracker Red CMXRos and MitoTracker Green under basal or MP stimulated conditions. (Q) Graph of MitoTracker Green-positive macrophages stimulated with or without microplastics. Representative of two to three independent experiments, Graphs indicate mean (±SD). ** P<0.01, ***P<0.001. Two-tailed unpaired Student's t test.